

Extensive spectral tuning of the proton transfer emission from 550 to 675 nm *via* a rational derivatization of 10-hydroxybenzo[*h*]quinoline†

Kew-Yu Chen, Cheng-Chih Hsieh, Yi-Ming Cheng, Chin-Hung Lai and Pi-Tai Chou*

Received (in Cambridge, UK) 18th July 2006, Accepted 18th August 2006

First published as an Advance Article on the web 15th September 2006

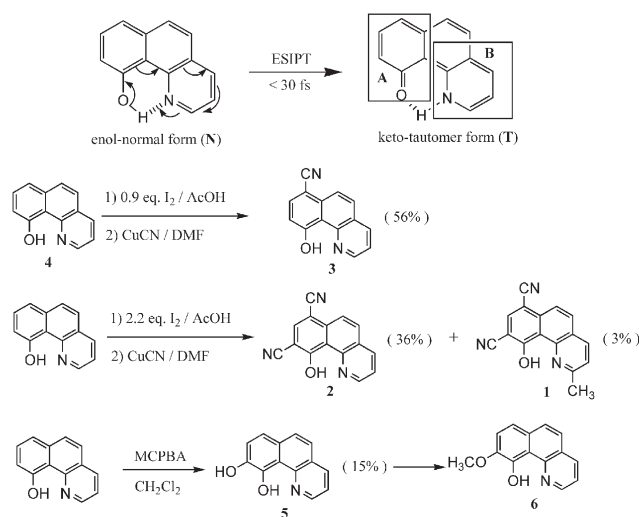
DOI: 10.1039/b610274c

Via a systematic derivatization of the excited-state intramolecular proton-transfer system, 10-hydroxybenzo[*h*]quinoline, the proton-transfer emission can be extensively tuned from 550 nm (1) to 675 nm (6), in which amplified spontaneous emission was readily observed for 1–3, generating a new family of proton transfer laser dyes.

The fundamental approach to a proton transfer process, which is crucial to many chemical and biological reactions, has relied deeply on studies of the excited-state intramolecular proton transfer (ESIPT) reaction.¹ The ESIPT reaction generally incorporates transfer of a hydroxyl (or amino) proton to the carbonyl oxygen (or pyridyl nitrogen) through a pre-existing hydrogen bonding configuration. The resulting proton-transfer tautomer possesses significant differences in structure and electronic configuration from its corresponding normal species. Accordingly, a large Stokes shifted $S'_1 \rightarrow S'_0$ fluorescence (hereafter, the prime sign denotes the proton-transfer tautomer) was observed. This unusual photophysical property has found many important applications. Prototypical examples are probes for solvation dynamics² and biological environments,³ the development of laser dyes,^{4–6} fluorescence recording,^{7,8} ultraviolet stabilizers,⁹ metal ion sensors,¹⁰ radiation hard-scintillator counters¹¹ and recent application in the field of organic light emitting devices (OLEDs).¹²

From the application viewpoint, one important issue regarding the ESIPT system lies in the wide tunability of the proton transfer emission. Most of the ESIPT molecules possess the $S_0 \rightarrow S_1$ transition band around near UV, while upon excitation, the occurrence of ESIPT gives rise to visible emissions. It is thus expected that a UV source such as a GaN laser may be suited to pumping a combination of ESIPT systems containing RGB colors without mutual interference, achieving white light generation. Such a perspective makes the ESIPT systems versatile in the many potential applications listed above.

Bearing this aim in mind, we have screened numerous ESIPT molecules and strategically selected 10-hydroxybenzo[*h*]quinoline (HBQ) as a prototype.^{13,14} Owing to the intrinsic six-membered ring hydrogen bond, HBQ serves as perhaps the most prominent ESIPT system that undergoes an ultrafast (<30 fs) proton transfer free from the solvent perturbation.^{15,16} Moreover, its great photostability and number of fused rings accessible for chemical modification lead to further derivations being feasible. As depicted



Scheme 1

in Scheme 1, due to its in-built aromaticity, in which the π electrons are extensively delocalized, the substituent effect on the normal species (enol form N, see Scheme 1) is expected to be small due to a simultaneous perturbation on both HOMO and LUMO levels. Conversely, the occurrence of ESIPT, forming a keto-tautomer (T) species, should be accompanied by a charge transfer event from the phenolic ring to the pyridine ring (see Scheme 1). One can thus consider the keto-tautomer moiety to be composed of two segments: the HOMO and LUMO parts located at cyclohexa-2,4-dienone (the A moiety, see Fig. 1) and methylenepyridine

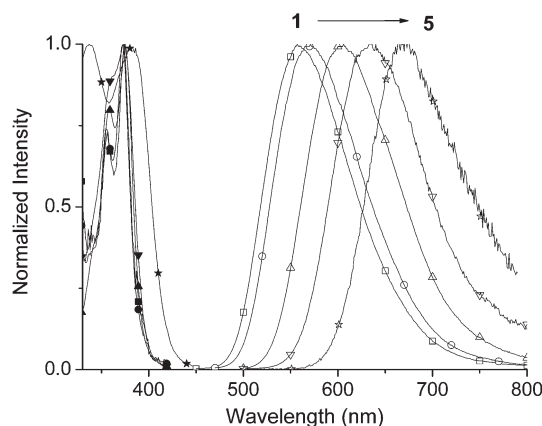


Fig. 1 The normalized absorption and emission spectra of 1 (■) (□), 2 (●) (○), 3 (▲) (△), 4 (▼) (▽), 5 (★) (☆) in ethyl acetate.

Department of Chemistry, National Taiwan University, Taipei, 106, Taiwan E-mail: chop@ntu.edu.tw; Fax: +886 (2) 2369 5208; Tel: +886 (2) 2364 3876 ext. 3988

† Electronic supplementary information (ESI) available: Detailed syntheses and characterization and measurements. See DOI: 10.1039/b610274c

(the **B** moiety), respectively. Adding an *e.g.* electron withdrawing substituent at the **A** moiety should result in a decrease of HOMO, hence the increase of an energy gap of the keto-tautomer emission. A similar substitution at the **B** moiety should cause a decrease of LUMO, hence the decrease of the energy gap of the keto-tautomer. An opposite effect is expected for the case of adding electron donating substituents. As a result, we expect a wide tunable range of the proton-transfer tautomer emission, while the parent ESIPT skeleton, *i.e.* HBQ, remains intact. In other words, fine-tuning of the proton transfer emission can be achieved with a small spectral alternation of the normal (N) absorption profile.

Scheme 1 depicts various synthetic routes to achieve compounds **1–3**, **5** and **6**. Under a stoichiometric control of I_2 , the iodination of HBQ, followed by the cynation of the monoiodo-HBQ and diiodo-HBQ, gave compounds **3** and **2**, respectively. To our surprise, we also isolated an unexpected compound **1**, which contained 7,9-dicyano substituents and a methyl group at the 2-position. The source of the methyl group has not been confirmed, but the solvent (acetic acid or DMF) could plausibly be the major supplier. The hydroxylation at 9-position of HBQ was achieved by the reaction of HBQ with 3-chloroperoxybenzoic acid, giving **5** with a yield of 15% after purification. Further methylation of **5** using dimethyl sulfate in 1,4-dioxane in the basic condition gave **6** with 90% yield. Detailed synthetic procedures and the corresponding structural characterization are elaborated in the ESI.†

Fig. 1 depicts the steady state absorption and emission spectra of **1–5** in ethyl acetate. For clarity, the emission spectrum of **6** is omitted in Fig. 1 because the difference between **5** and **6** is small (see Table 1). Despite the similarity in absorption spectra, in which the $S_0 \rightarrow S_1$ peak wavelengths are all located at 380–390 nm for **1–6**, the corresponding emission reveals remarkable differences. The emission peak greatly shifts from 550 nm in **1** to 675 nm in **6** in ethyl acetate. For **1–6**, the occurrence of ESIPT is supported by the anomalously large Stokes shifted emission with respect to the absorption peak wavelength.^{13,14} The lack of any enol-normal emission implies an ultrafast rate of ESIPT, the conclusion of which has been firmly supported by the femtosecond dynamics in compound **4**.^{15,16} The tendency of the spectral shift confirms the aforementioned empirical approach based on the interplay between the HOMO and LUMO, in which the addition of an electron withdrawing (donating) group at the phenol site decreases (increases) the HOMO level and hence increases (decreases) the keto-tautomer energy gap, while adding the donating group ($-\text{CH}_3$) at the pyridyl site raises the LUMO and hence increases the energy gap. This viewpoint can be further supported by a theoretical approach based on time-dependent density function theory (TDDFT, see ESI†). Taking compound **1** as an example, as depicted in Fig. 2, significant differences in the frontier orbital configuration can be promptly viewed between enol-normal and

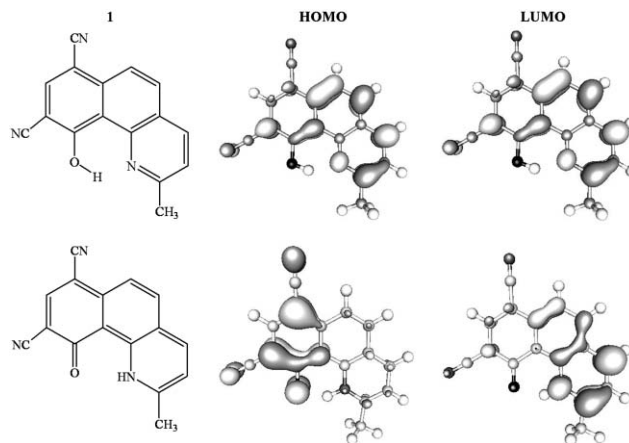


Fig. 2 The calculated HOMO and LUMO molecular orbitals of normal and tautomer form of **1** (Gaussian 03 HF/6-31++G(d,p'), see ESI†).

keto-tautomer forms. For the enol form, the π electron density, to a great extent, is spread over the entire framework for both HOMO and LUMO. In sharp contrast, the HOMO and LUMO for the keto-tautomer form are substantially located at cyclohexa-2,4-dienone (the **A** moiety, see Fig. 1) and methylenepyridine (the **B** moiety), respectively, consistent with the experimental results.

As shown in Table 1, intriguing photophysical properties are observed among **1–6**, for which the tautomer emission yield reveals a decreasing tendency upon lowering of the emission gap. For the $S'_1 \rightarrow S'_0$ deactivation process, as an empirical approach (*i.e.* energy gap law),¹⁷ in the absence of a zero-order surface crossing between S_1 and S_0 states, the rate constant of an $S'_1 \rightarrow S'_0$ internal conversion can be estimated by $\nu \exp(-\alpha \Delta E)$ where α is a proportionality constant and ΔE denotes the emission energy gap. The non-radiative decay rate k_{nr} can be deduced from $k_{nr} = k_{obs} - k_r$, in which k_{obs} and k_r denote the observed and radiative decay rate constants, respectively. k_r can be further deduced by $k_r = k_{obs} \Phi$, in which Φ specifies the emission quantum yield. As depicted in Fig. 3, the plot of $\ln(k_{nr})$ vs. the energy gap ΔE (in kcal mol⁻¹) gives a sufficiently straight line, with ν calculated to be $\sim 10^{14}$ s⁻¹, respectively, supporting the matching type of radiationless deactivation for the tautomer emission of **1–6**.

Owing to a reversible four-electronic level reaction, the ESIPT system renders an ideal basis to achieve the lasing action.⁴ This, in combination with the relatively high fluorescence yields of **1–3**, led

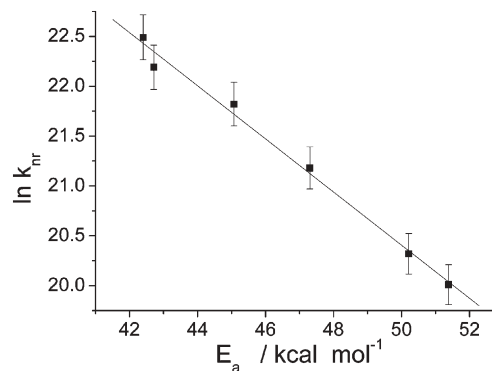


Fig. 3 The plot of $\ln(k_{nr})$ vs. the energy gap ΔE , in which ΔE was taken to be the emission peak in terms of kcal mol⁻¹.

Table 1 Steady-state photophysical properties of **1–6** in ethyl acetate

| | $\lambda_{abs}^{max}/\text{nm}$ | $\lambda_{em}^{max}/\text{nm}$ | τ/ns | Φ |
|----------|---------------------------------|--------------------------------|------------------|--------|
| 1 | 374 | 550 | 1.13 | 0.45 |
| 2 | 373 | 570 | 1.05 | 0.31 |
| 3 | 375 | 605 | 0.66 | 0.13 |
| 4 | 374 | 635 | 0.33 | 0.02 |
| 5 | 380 | 670 | 0.23 | 0.009 |
| 6 | 380 | 675 | 0.17 | 0.003 |

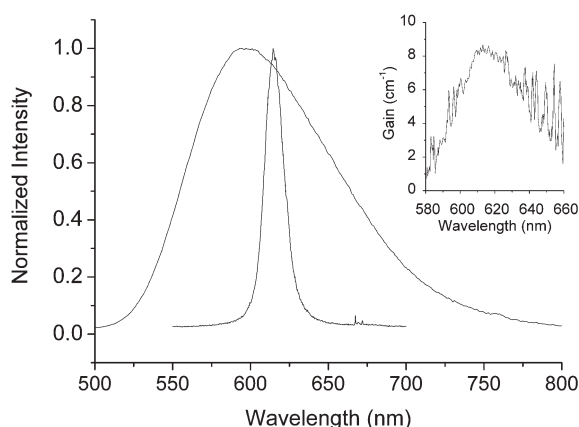


Fig. 4 The emission and ASE of **3** in dichloromethane. Inset: The deduced gain spectrum. λ_{ex} : 380 nm.

us to examine the possibility of lasing properties through the measurement of amplified spontaneous emission (ASE). We chose compound **3**, which had the lowest emission yield among **1–3**, 0.13, to demonstrate the power of lasing action for this ESIPT system. In this experiment, optical gain measurements were carried out using the variable stripe length method.¹⁸ The second harmonic (380 nm, pulse width 8 ns) of a Q-switched Nd:YAG pumped Ti:sapphire laser was focused into a stripe on the quartz cell by a cylindrical lens. The stripe length was adjusted by a barrier coated with opaque materials. The stripe was aligned near the edge of the square quartz cell, and the emission was collected from the edge at a 90° angle with respect to the excitation beam. The emission was analyzed using a polychromator coupled to an intensified charge coupled detector.

Fig. 4 shows the ASE spectra of **3** in dichloromethane. The exponential dependence of the intensity of the ASE on the gain coefficient $\alpha(\lambda)$ leads to the observed band narrowing. By measuring the intensity I_L of ASE from the entire cell length L and the intensity $I_{L/2}$ from the cell half-length, one can evaluate the ASE gain $\alpha(\lambda)$,¹⁹ expressed as

$$\alpha(\lambda) = (2/L)\ln[(I_L/I_{L/2}) - 1]$$

The gain spectrum is obtained from the analysis of the spectroscopic data recorded using the above equation. As shown in the inset of Fig. 4, the experimental gain spectrum of **3** in CH₂Cl₂ at a pump power of 10 mW covered a region from ~590 to 640 nm, with a maximum at 615 nm and a gain efficiency of ~9.0, which is comparable with many other commercially available laser dyes. The lack of reabsorption at the ASE region is believed to play a key factor for observing the stimulating emission. Similar ASEs were obtained for **1** and **2**, with ASE peak wavelengths at 565 and 582 nm, respectively, generating a new series of ESIPT laser dyes in the green–red region.

In conclusion, on the basis of the ESIPT system HBQ, we have systematically synthesized a new series of derivatives, such that the proton-transfer emission can be extensively tuned from 550 nm (**1**) to ~680 nm (**6**), the emission yield of which obeys the energy gap law. For the case of **1–3**, the emission quantum yield was measured to be >0.13 in ethyl acetate, and ASE was readily observed, generating a new family of proton transfer fluorescence dyes. Future applications of this series of ESIPT molecules can be greatly expanded. For example, *via* mixing *e.g.* **1** ($\lambda_{\text{em}} \sim 550$ nm), **3** ($\lambda_{\text{em}} \sim 605$ nm) and the methoxylated derivative of **4**, in which ESIPT is prohibited (emission $\lambda_{\text{max}} \sim 420$ nm, $\Phi \sim 0.3$ in ethyl acetate),¹⁴ a qualitative white light generation can be achieved with a regular UV lamp (366 nm, see TOC). As for other examples, through the hydrolysis of cyano substituents, synthesis of water-soluble fluorescent dyes can be achieved, such that their applications toward fluorescent imaging and biomolecular recognition become feasible. Work focusing on this issue is currently in progress.

Notes and references

- For representative examples, see: (a) E. M. Kosower and D. Huppert, *Annu. Rev. Phys. Chem.*, 1986, **37**, 127; (b) Special Issue (Spectroscopy and Dynamics of Elementary Proton Transfer in Polyatomic systems, ed. P. F. Barbara and H. D. Trommsdorff), *Chem. Phys.*, 1989, **136**, 153; (c) W. S. Yu, C. C. Cheng, Yi. Ming. Cheng, P. C. Wu, Y. H. Song, Y. Chi and P. T. Chou, *J. Am. Chem. Soc.*, 2003, **125**, 10800; (d) S. F. Formosinho and L. G. Arnaut, *J. Photochem. Photobiol., A: Chem.*, 1993, **75**, 21; (e) S. Scheiner, *J. Phys. Chem. A*, 2000, **104**, 5898; (f) J. Waluk, *Acc. Chem. Res.*, 2003, **36**, 832.
- F. Parsapour and D. F. Kelley, *J. Phys. Chem.*, 1996, **100**, 2791.
- A. Sytnik and M. Kasha, *Proc. Natl. Acad. Sci. USA*, 1994, **91**, 8627.
- P. T. Chou, D. McMorro, T. J. Aartsma and M. Kasha, *J. Phys. Chem.*, 1984, **88**, 4596.
- A. V. Acuna, F. Amat-Guerri, J. Catalán, A. Costella, J. Figuera and J. Munoz, *Chem. Phys. Lett.*, 1986, **132**, 576.
- K. I. Sakai, T. Tsuzuki, Y. Itoh, M. Ichikawa and Y. Taniguchi, *Appl. Phys. Lett.*, 2005, **86**, 081103.
- S. Kim and S. Y. Park, *Adv. Mater.*, 2003, **15**, 1341.
- S. Kim, S. Y. Park, I. Tashida, H. Kawai and T. Nagamura, *J. Phys. Chem. B*, 2002, **106**, 9291.
- J. Catalán, J. C. del Valle, R. M. Claramunt, D. Sanz and J. Dotor, *J. Lumin.*, 1996, **68**, 165.
- A. D. Roshal, A. V. Grigorovich, A. O. Doroshenko and V. G. Pivovarenko, *J. Phys. Chem. A*, 1998, **102**, 5907.
- C. L. Renschler and L. A. Harrah, *Nucl. Instrum. Methods Phys. Res., Sect. A*, 1985, **235**, 41.
- S. Kim, J. Seo, H. K. Jung, J. J. Kim and S. Y. Park, *Adv. Mater.*, 2005, **17**, 2077.
- M. L. Martinez, W. C. Cooper and P. T. Chou, *Chem. Phys. Lett.*, 1992, **193**, 151.
- P. T. Chou and C. Y. Wei, *J. Phys. Chem.*, 1996, **100**, 17059.
- P. T. Chou, Y. C. Chen, W. S. Yu, Y. H. Chou, C. Y. Wei and Y. M. Cheng, *J. Phys. Chem. A*, 2001, **105**, 1731.
- S. Takeuchi and T. Tahara, *J. Phys. Chem. A*, 2005, **109**, 10199.
- W. Siebrand, *J. Chem. Phys.*, 1967, **47**, 2411.
- K. L. Shaklee, R. E. Nahory and R. F. Leheny, *J. Lumin.*, 1973, **7**, 284.
- (a) W. T. Silfvast and J. S. Deech, *Appl. Phys. Lett.*, 1967, **17**, 97; (b) O. G. Peterson, J. P. Webb, W. C. McColgin and J. H. Eberly, *J. Appl. Phys.*, 1971, **42**, 1917; (c) C. V. Shank, *Rev. Mod. Phys.*, 1975, **47**, 649.